

Near-field observation of spatial phase shifts associated with Goos-Hänschen and Surface Plasmon Resonance effects

J. Jose*, F. B. Segerink, J. P. Korterik and H. L. Offerhaus

*Optical Sciences group, MESA⁺ Institute for Nanotechnology,
University of Twente, 7500 AE, Enschede, The Netherlands*

j.jose@utwente.nl

Abstract: We report the near-field observation of the phase shifts associated with total internal reflection on a glass-air interface and surface plasmon resonance on a glass-gold-air system. The phase of the evanescent waves on glass and gold surfaces, as a function of incident angle, is measured using a phase-sensitive Photon Scanning Tunneling Microscope (PSTM) and shows a good agreement with theory.

© 2008 Optical Society of America

OCIS codes: (240.0240) Optics at surfaces; (120.5050) Phase measurement; (180.4243) Near-field microscopy; (240.6680) Surface plasmons

References and links

1. I. Newton, *Opticks* (William Innys, London, 1704).
2. N. J. Harrick, *Internal reflection spectroscopy* (Interscience Publishers, New York (0-470-35250-7) 1967).
3. R. C. Reddick, R. J. Warmack, and T. L. Ferrell, "New form of scanning optical microscopy," *Phys. Rev. B* **39** (1989).
4. A. Lewis, H. Taha, A. Strinkovski, A. Manevitch, A. Khatchaturiants, R. Dekhter, and E. Ammann, "Near-field optics: from subwavelength illumination to nanometric shadowing," *Nature Biotechnol.* **21** (2003).
5. R. Quidant, J. C. Webber, A. Dereux, D. Payrade, Y. Chen, and G. Girard, "Near-field observation of evanescent light wave coupling in subwavelength optical waveguides," *Europhys. Lett.* **57** (2002).
6. F. Goos and H. Hänchen, "Ein neuer und fundamentales versuch zur total reflexion," *Ann. Phys.* **1** (1947).
7. R. H. Ritchie, "Plasma losses by fast electrons in thin films," *Phys. Rev.* **1** (1957).
8. S. G. Nelson, K. S. Johnston, and S. S. Yee, "High sensitivity surface plasmon resonance sensor based on phase detection," *Sens. Actuators B* **35** (1996).
9. S. A. Shen, T. Liu, and J. H. Guo, "Optical phase-shift detection of surface plasmon resonance," *Appl. Opt.* **37** (1998).
10. V. E. Kochergin, A. A. Beloglazov, M. V. Valeiko, and P. I. Nikitin, "Phase properties of a surface-plasmon resonance from the viewpoint of sensor applications," *Quantum Electron.* **28** (1998).
11. F. Pillon, H. Gilles, S. Girard, M. Laroche, and O. Emile, "Transverse displacement at total reflection near the grazing angle: a way to discriminate between theories," *Appl. Phys. B* **80** (2005).
12. H. P. Ho, W. W. Lam, and S. Y. Wu, "Surface plasmon resonance sensor based on the measurement of differential phase," *Rev. Sci. Instrum.* **73** 2002.
13. X. B. Yin and L. Hesselink, "Goos-hanchen shift surface plasmon resonance sensor," *Appl. Phys. Lett.* **89** (2006).
14. C. F. Li, T. Duan, and X. Y. Yang, "Giant Goos-Hanchen displacement enhanced by dielectric film in frustrated total internal reflection configuration," *J. Appl. Phys.* **101** (2007).
15. P. I. Nikitin, A. A. Beloglazov, V. E. Kochergin, M. V. Valeiko, and T. I. Ksenevich, "Surface plasmon resonance interferometry for biological and chemical sensing," *Sens. Actuators B* **54** (1999).
16. H. P. Chiang, J. L. Lin, and Z. W. Chen, "High sensitivity surface plasmon resonance sensor based on phase interrogation at optimal incident wavelengths," *Appl. Phys. Lett.* **88** (2006).
17. K. M. Medicus, M. Chaney, J. E. Brodziak, and A. Davies, "Interferometric measurement of phase change on reflection," *Appl. Opt.* **46** (2007).
18. S. Kaiser, T. Maier, A. Grossmann, and C. Zimmermann, "Fizeau interferometer for phase shifting interferometry in ultrahigh vacuum," *Rev. Sci. Instrum.* **72** (2001).

19. E. Kretschmann and H. Raether, "Radiative decay of nonradiative surface plasmons excited by light," *Z.Naturforsch.A* **23** (1968).
20. E. Hecht, *Optics* (Addison Wesley (0-201-83887-7) 1998).
21. C.K. Carniglia and L. Mandel, "Phase-shift measurement of evanescent electromagnetic waves," *J. Opt. Soc. Am.* **61** (1971).
22. K. Kiersnowski, L. Jozefowski, and T. Dohnalik, "Effective optical anisotropy in evanescent wave propagation in atomic vapor," *Phys. Rev. A* **57** (1998).
23. H. Raether, *Surface Plasmons on Smooth and Rough Surfaces and on Gratings* (Springer, Berlin (3-540-17363-3) 1988).
24. F. de Fornel, P. M. Adam, L. Salomon, J. P. Goudonnet, A. Sentenac, R. Carminati, and J. J. Greffet, "Analysis of image formation with a photon scanning tunneling microscope," *J. Opt. Soc. Am. A* **13** (1996).
25. M. L. M. Balistreri, J. P. Korterik, L. Kuipers, and N. F. van Hulst, "Local observations of phase singularities in optical fields in waveguide structures," *Phys. Rev. Lett.* **85** (2000).
26. P. Mazur and B. Djafarirouhani, "Effect of surface-polaritons on the lateral displacement of a light-beam at a dielectric interface," *Phys. Rev. B* **30** (1984).

1. Introduction

Newton demonstrated, with the help of a glass of water, that total internal reflection (TIR) at an interface separating two media can be inhibited and predicted the existence of evanescent waves in the optically rarer medium [1, 2]. This demonstration paved the way for the development of the entire field of internal reflection microscopy. The evanescent waves are non-radiative and bound close to the surface where they are generated. Probing these evanescent waves reveals the behavior of light at the interface in the near field [3, 4, 5]. In 1947, Goos and Hänchen performed a more detailed analysis of Newton's prediction and experimentally demonstrated a lateral displacement of the total internally reflected beam, thereafter known as the "Goos-Hänchen effect" (GHE) [6].

A similar phenomenon on a metal-dielectric interface occurs due to the creation of "Surface Plasmon Polaritons" (SPP) [7]. SPPs are charge density waves that can be excited on a metal-dielectric interface when the resonance condition is met: the in-plane wave vector component (k_x) of the incident light matches the SPP wave vector (k_{sp}) [8]. The distinct absorption dip and the sharp phase variation at a Surface Plasmon Resonance (SPR) have been extensively studied [8, 9, 10]. The phase shift associated with both the GHE and the SPR have been independently studied in the past [11, 12]. It has already been shown that SPPs can be used to enhance the GHE [13, 14]. Such an enhancement of the GHE due to material resonances has applications in the field of SPR sensors [8, 15, 16]. A recent interferometric study reported a measurement of the difference between the phase shift upon reflection off a glass-gold interface and that off a glass-air interface at normal incidence in the far field using a back reflection geometry [17]. In order to observe this phase shift locally, here we probe the evanescent waves generated at the interface. We show near-field measurements of the spatial phase shift of optical fields across the glass-gold transition region as a function of incident angle using a phase-sensitive Photon Scanning Tunneling Microscope (PSTM).

Unlike time-varying phase-shifting interferometry [18], we use a position varying technique where the spatial phase evolution of evanescent waves on surfaces with different optical constants is observed simultaneously. Evanescent waves were generated by TIR on a glass-air interface and SPPs by Kretschmann-Raether configuration [19] in a glass-gold-air stack as illustrated in Fig. 1(a). We exploit the unique property of evanescent waves that the surfaces of constant amplitude (parallel to the plane of the interface) are perpendicular to the surfaces of constant phase (normal to the plane of the interface). Since they do not coincide, the propagating surface wave is inhomogeneous [20]. In other words there is no propagation in a direction perpendicular to the interface. Instead, the wave propagates parallel to the interface with a definite wavelength component $\lambda_x = 2\pi/k_x$ where k_x is the in-plane wave vector component given by

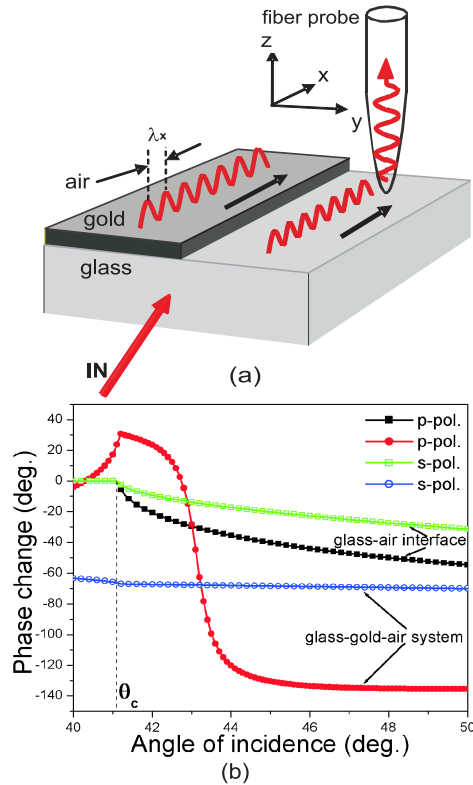


Fig. 1. (a) Schematic illustration of our approach (b) Calculated phase change with respect to incoming beam obtained from the Fresnel's coefficients as a function of incident angle for both a glass-air interface (squares) and a glass-gold-air system (circles). The abrupt variation in phase change for the p-polarized incident beam in the glass-gold-air system (red) is due to the excitation of surface plasmons. θ_c is the critical angle of incidence for TIR on the glass-air interface

$k_x = k_i \sin \theta_i$ where θ_i is the angle of incidence and k_i is the wave number of the incident beam. Upon introducing a sharp tapered optical fiber tip into the evanescent wave region, frustrated TIR occurs and a small part of the evanescent waves propagates into the fiber [5]. Owing to the inhomogeneous nature of evanescent waves, the phase change upon evanescent wave coupling into the fiber, across an air gap, is independent of the width of the gap [21]. By raster scanning the sample surface using the fiber tip, the spatial evolution of the phase of evanescent waves on the surface of the sample is observed. The different optical constants for glass and gold as well as the thin layer of gold on the glass surface induces a stationary difference between phases of

the evanescent waves on the glass-air interface and on the glass-gold-air stack. In addition to this constant phase difference, there are two other significant phase changes that vary with θ_i : one associated with the GHE on the glass-air interface and another with the SPR on the glass-gold-air system. The phase change at the SPR occurs only when the incident beam is polarized parallel (p) to the plane of incidence; not for polarization perpendicular (s) to the plane of incidence. In contrast, the phase change associated with GHE occurs for both the polarizations, but is different for p and s polarization [22]. Theoretical plots of phase change for p- and s-polarized incident beams as a function of incident angle obtained from Fresnel's reflection and transmission coefficients [23] for glass/air and glass/gold/air systems are shown in Fig. 1(b).

2. Experimental

Our samples are commercially available gold SPR sensors (Ssens) with a titanium adhesive layer on a glass substrate of thickness 0.3 mm. The thickness of the gold layer is approximately 50 nm. Using Focused Ion Beam (FIB) milling, a glass 'window' on the sample is made by removing $50 \times 500 \mu\text{m}^2$ strip of gold. Technical constraints on the focused ion beam milling of the gold made it impossible to remove the gold completely from the glass surface and hence traces of gold remain. The region of our interest is the transition from gold to glass. The structure is placed on top of a glass (BK7) hemispherical prism with index matching oil in between. A fiber collimator focuses the laser light to the glass-gold transition region of the sample and is mounted on a goniometric stage for angles ranging from 40° to 50° . The divergence of the beam introduces a convolution error of less than 1° in the angle of incidence. We selected a sample configuration where the sample is oriented in such a way that the gold 'step' is parallel to the plane of incidence so that reflection effects due to the gold step are eliminated [24].

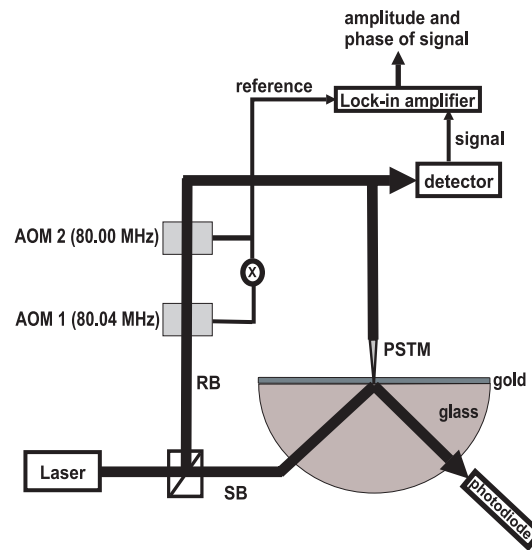


Fig. 2. Schematic diagram of the phase-sensitive PSTM with the sample placed on top of a glass hemispherical prism (side view). SB - signal branch, RB - reference branch

The operating principle of a phase-sensitive PSTM has already been reported in detail before [25]; but we will summarize its method of operation. A schematic is shown in Fig. 2. The incoming laser beam (He-Ne; $\lambda = 632.8\text{nm}$) is split into a signal branch that illuminates the sample, and a reference branch which is shifted in frequency by 40 kHz using two acousto-optic modulators. The reference beam interferes with the small signal picked up by the probe and is

measured by a detector, generating a signal at 40 kHz. This signal is proportional to the optical amplitude picked up by the fiber tip (E_s) as well as the optical amplitude in the reference branch (E_r), and is measured with a dual-phase Lock-in-Amplifier (LIA) locked to 40 kHz. The phase of the detected signal depends on the phase of the local field on the sample surface compared to the phase of the reference branch. The LIA provides optical amplitude ($E_s E_r$), optical amplitude times cosine of the relative phase of local field ($E_s E_r \cos(\phi)$) and optical amplitude times sine of the relative phase of local field ($E_s E_r \sin(\phi)$). The distance between the fiber tip and the sample surface is kept constant throughout the scanning using shear-force feedback. Thus local optical phase on the sample surface as a function of position and topographical information are simultaneously retrieved.

3. Results and discussion

A typical PSTM measurement for an s-polarized incident beam is presented in Fig. 3. Figure 3(a) shows the topography of the sample. Figure 3(b) shows the optical amplitude times sine of the relative phase of the local field. The spacing between adjacent dark or bright lines is a direct measurement of the wavelength component λ_x on the sample surface.

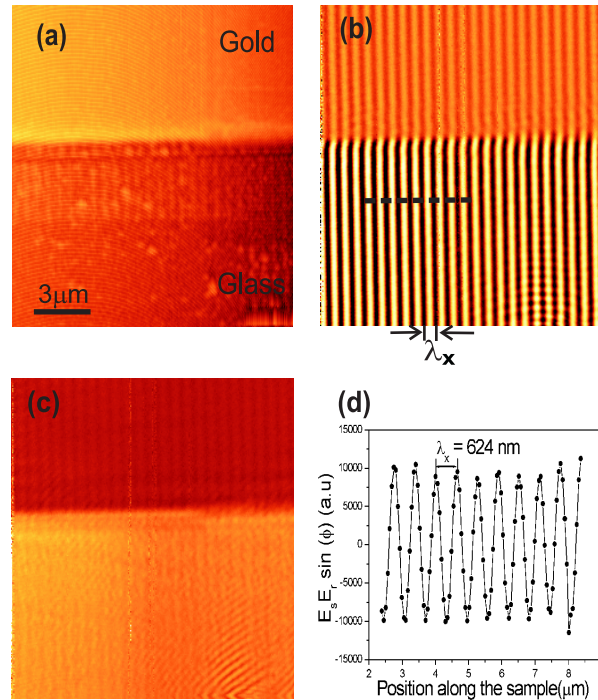


Fig. 3. A PSTM measurement of the glass-gold transition region of the sample for a scan area of $24.1 \times 14.8 \mu m^2$ for an s-polarized incident beam. (a) Topography, (b) phase of the local field expressed as optical amplitude times sine of the phase, (c) the measured amplitude of the optical field, (d) a line trace on the sample along the black dashed line in image (c). The images were obtained using a coated fiber tip.

The parallel and equidistant phase fronts (Fig. 3(b)) support the stability of our interferometric setup. Figure 3(c) shows the optical amplitude ($E_s E_r$) obtained from the output of the LIA. Since the tip to sample distance is kept constant, the optical amplitude is uniform above each interface. We see a lower optical amplitude on the gold region which is due to lower transmis-

sion in the absence of surface plasmons. Figure 3(d) shows a line profile taken across the phase fronts shown as a black dotted line on the glass part in Fig. 3(c).

PSTM images depicting the evolution of the shift in spatial phase across the glass-gold transition region of the sample for the p-polarized incident beam are shown in Fig. 4. As the incident angle varies from 42.2° to 43.6° (Fig. 4(b)-(e)), the shift in the spatial phase on the boundary separating the glass and gold regions changes. The rate of change has a maximum in the SPR region. Using a two dimensional Fast Fourier Transform, the phases on the gold and glass regions of the sample were extracted for incident angles ranging from 40° to 50° . The difference between these phases plotted against incident angle is shown in Fig. 5(a), together with the difference between the theoretical phase changes which are shown in Fig. 1(b).

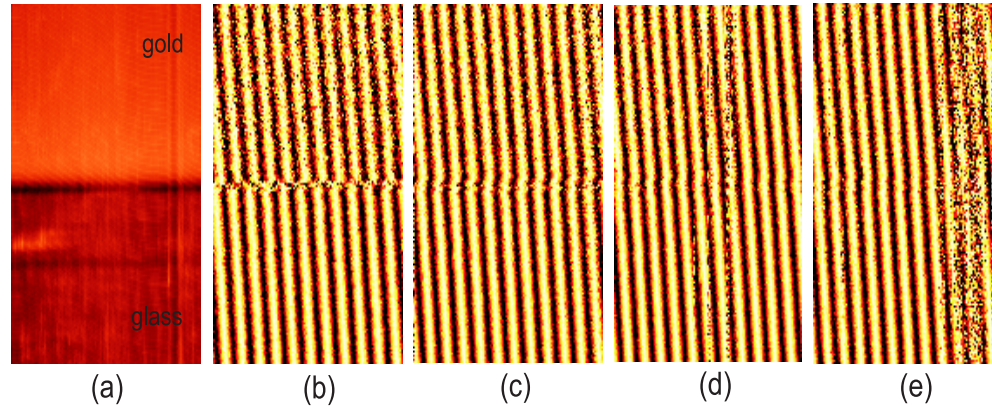


Fig. 4. PSTM images for a p-polarized incident beam and a scan area of $60 \times 6.4 \mu\text{m}^2$. (a) Topography, (b-e) the sine of the spatial phase for different incident angles (b) 42.2° , (c) 42.7° , (d) 43.3° , (e) 43.6° . The images were obtained using a coated fiber tip.

The change in measured phase difference is 130° , which agrees well with the theory and is caused mainly by the enhanced spatial phase shift on the glass-gold-air system due to the generation of SPP. This enhanced spatial phase shift corresponds to an increased GHE [26] of $3.5 \mu\text{m}$ as defined in [14]. Interestingly, we see an offset in the phase difference measured using a coated fiber tip compared to that measured using an uncoated fiber tip for both p- and s-polarized incident beams. The interaction between the metal coated probe and the surface might introduce an additional phase shift for the entire range of incident angles. This may explain the offset observed; but is not a relevant issue of concern in this study. We performed simultaneous far-field reflectivity studies to cross-check the generation of plasmons using a photodiode (as shown in Fig. 2) that detects the light reflected off the glass-gold-air system. The absorption dip in the reflectivity measurements for the p-polarized light clearly indicates the SPR angle as 43.3° . Figure 5(b) shows a comparison between reflectivity and PSTM measurements. The distinct change in the phase difference of 130° is measured over the SPR range for the p-polarized light, whereas for the s-polarized light a negligible change is measured over the SPR region as expected. We do see a minor fluctuation in the reflected signal voltage which we attribute to polarization impurity. This impurity leads to a similar fluctuation in the corresponding phase difference plot. It has been reported that a change in the ambient refractive index influences the SPR so that the angular position of the phase difference for p-polarized incident beam would move along the *angle of incidence* axis [15]. Note that the angular position of the measured change in phase difference for p-polarized incident beam coincides with the absorption dip in the plot obtained from reflectivity measurement. This observation underlines the fact that the measured change in phase difference is not influenced by the presence of a near-field optical

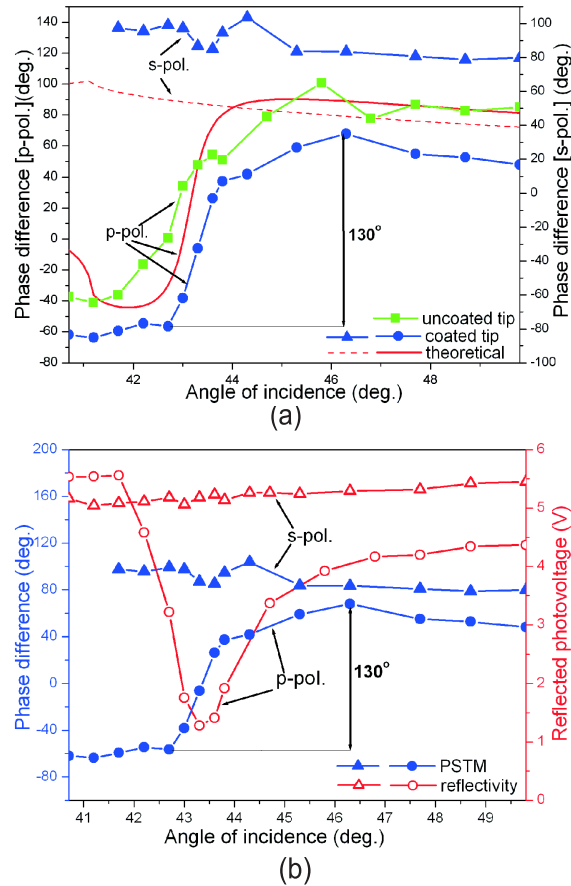


Fig. 5. (a) Comparison between the theoretical and experimental phase difference as a function of incident angle for p- and s- polarized light. (b) Comparison between far-field reflectivity and near-field PSTM measurements for p- and s- polarized incident beams.

fiber tip.

4. Summary

In conclusion, we have observed the shift in the spatial phase of evanescent waves on glass-air and glass-gold-air systems as a function of incident angle locally using a phase-sensitive PSTM. Our observations are the first of this kind in the near-field, which measure the spatial phase shift associated with GHE and SPR on the surface. The change in the phase difference of the evanescent waves across the glass-gold transition region of the sample as a function of incident angle shows the combined effect of the GHE and the generation of surface plasmons and agrees well with the theoretical predictions. Our experiments on directly measuring the local optical phase of the SPP provides a new approach for the near-field SPR sensors.

It is a pleasure to thank Robert Moerland for fruitful discussions and Prof. Jennifer Herek for reviewing the manuscript. This research is supported by NanoNed, a nanotechnology program of the Dutch Ministry of Economic Affairs.